Research paper

Experimental study on shear mechanical properties of cement mortar specimen with through-step joints under direct shear

Liangxiao Xiong[1], Haijun Chen[2], Haogang Guo[3], Songhua Mei[4], Zhongyuan Xu[5], Bin Liu[6]

Abstract: In this study, direct shear tests were carried out on cement mortar specimens with single-ladder, single-rectangular, and double-rectangular step joints. Consequently, the shear strength, and crack shape of specimens with these through-step joints were analyzed, for understanding the influence of the through-step joint's shape on the direct shear mechanical properties. The results of the investigation are as follows: (1) Under the same normal stress, any increases in the height h of the step joint causes an initial-increase-decrease in the shear strengths of specimens with single-ladder and double-rectangular step joints, causing a type-W variation pattern for the specimens with single-rectangular step joint. More essentially, when normal stress and h are constant, the shear strength of specimens with a single-ladder step joint is the greatest, followed by specimens with a double-rectangular step joint, and then specimens with a single-rectangular step joint is the least. (2) Furthermore, given a small h and low normal stress, specimen with a single-ladder step joint mainly experiences shear failure, whereas specimens with single-rectangular and double-rectangular step joints mainly generate extrusion milling in the step joints.

Keywords: artificial rock specimen, ladder step joint, rectangular step joint, height of step joint, shear strength

---

[1]Associate Prof., PhD., Eng., Hunan Provincial Key Laboratory of Hydropower Development Key Technology, Power China Zhongnan Engineering Corporation Limited, Changsha 410014, China, e-mail: xionglx1982@126.com, ORCID: 0000-0002-6366-5187

[2]Prof., PhD., Eng., Geotechnical Engineering Department, Nanjing Hydraulic Research Institute, Nanjing, 210029, China, e-mail: hjchen@nhri.cn, ORCID: 0000-0003-0094-9649

[3]MSc., Eng., Civil and Environmental Engineering Department, Carnegie Mellon University, Pittsburgh 15289, United States, e-mail: 279151413@qq.com, ORCID: 0000-0002-0367-8998

[4]Prof., PhD., Eng., Hunan Provincial Key Laboratory of Hydropower Development Key Technology, PowerChina Zhongnan Engineering Corporation Limited, China, e-mail: 409118467@qq.com, ORCID: 0000-0002-6122-3967

[5]PhD., Faculty of Geosciences and Environmental Engineering, Southwest Jiaotong University, Chengdu 611756, China, e-mail: zyxu@swjtu.edu.cn, ORCID: 0000-0003-4303-1870

[6]BEng., School of Civil Engineering and Architecture, East China Jiaotong University, Nanchang 330013, China, e-mail: 2217882326@qq.com, ORCID: 0000-0002-8485-4200

1. Introduction

Actual engineering rock mass damage normally depends on the distribution law and shear strength characteristics of the joint plane. Indeed, this relation justifies why the joint plane's direct shear mechanical properties have always been a focus of research in rock mechanics.

Researchers have conducted multiple tests and numerical simulations on the direct shear mechanical properties of joint planes with a serrated shape. Yang & Chiang [1] performed direct shear test on two types of artificial joints with single tooth-shaped asperities at different inclined angles, and found that the shear stress-displacement curve of the composite joint displays a distinguishing twin-peak pattern. Ghazvinian et al. [2] investigated the shear behavior of discontinuities caused by bedding planes of weakness between two different rock types with large strength difference, and demonstrated that the shear behavior of discontinuities with different joint wall compressive strengths (JCS) is different from rock joints with identical wall compressive strengths. Mohammad et al. [3] simulated the mechanical behaviour of rock fracture profiles during direct shear tests by using the two-dimensional particle flow computer code, peak and residual shear strength values and failure modes of the simulated fractures are shown to well represent the results obtained in laboratory tests and by analytical solutions. He et al. [4] conducted analytical and numerical solutions for shear mechanical behaviors of structural plane, and found that structural plane presents nonlinear characteristics. Bahaaddini et al. [5] studied the shear behaviour and mechanisms of asperity degradation of rock joints under direct shear tests using numerical and experimental approaches, and three shearing mechanisms of sliding, asperity surface wear and asperity shearing off were observed in both experimental and numerical tests. Mahdi Niktabar et al. [6] conducted cyclic shear tests on regular and irregular joints with different asperity angles, and the results indicate that the shear strength of rock joint increases with increase in asperity angle. Tian et al. [7] carried out 3D scanning and direct shear tests for 10 groups of grouted joint specimens, and found that the damage to grouted joints is markedly different from that of the un-grouted joints after shearing. Zhang et al. [8] studied degradation characteristics and mechanical properties of rock joints based on direct shear tests on six groups of artificial rock joints with regular profiles, and found that the fracture characteristics of the surface asperity were classified in three progressive change steps. Xiong et al. [9] conducted the shear behavior of artificial jointed rock samples with parallel joints using direct shear tests, and found that the entire shear process of non-coplanar intermittent joints generally consists of five stages. Xiong et al. [10] conducted direct shear tests on cement mortar samples with symmetrical and asymmetric toothed structural joints, and found that the types of shear failure modes of the joint plane primarily include root cutting, extrusion milling to spalling for the through-symmetrical and -asymmetrical toothed structural planes. Hao et al. [11] conducted cyclic direct shear test on rock sample with stepped structural plane, and found that the shear strength of the stepped structural plane and the deterioration index of shear strength are affected by the stress concentration at the corners of the structural plane and the length of the rock bridge of the specimen.

There are also several studies carried out direct shear tests on rock specimen with flat joint plane. Yang & Kulatilake [12] investigated the effect of the normal stress and joint

persistency on the mechanical behavior of granite samples containing discontinuous joints in the laboratory through direct shear tests, and the test results revealed three different failure modes occurring at the rock bridge. Cui [13] conducted direct shear tests to investigate the shear behavior of continuous planar joints, stepped joints, and discontinuous open joints, and found that the shear behavior of both the continuous and discontinuous joints has been found to be dependent on the normal stress. Xiong et al. [14] conducted direct shear tests of cement mortar samples with non-persistent planar joints, and found that the shear stress-shear displacement curve of samples with non-persistent planar joint under direct shear stress consists of five stages.

In actual engineering rock mass, the shape of a joint plane may be serrated, straight, step type, or rectangular. The first two types are common topics of current research studies involving the direct shear mechanical properties of joint planes, whereas studies for stepped or rectangular joint planes are relatively rare. For example, Kwon et al. [15] analyzed the shear behavior of rectangular asperities on rock joints, and results show that a joint with different asperity sizes experiences progressive failure in the order of asperity size, while a joint of identical asperity sizes approaches failure simultaneously.

In order to understand the influence of the shape of the through-step joint on the direct shear mechanical properties of jointed rock mass, this study focuses on direct shear tests applied on cement mortar specimens containing single-ladder, single-rectangular, and double-rectangular step joints. It gives details on the analysis of the shear strength and crack shape of specimens in each through-step joint, and describes how the through-step joint shape affects the direct shear mechanical properties of the cement mortar specimen.

2. Experimental setup

2.1. Specimen preparation

Cement mortar was the model material used in the test. No. 325 Portland cement produced by China Building Materials Academy was used, and the sand was mainly quartz sand. A specimen with a joint plane (dimension: 100 mm × 100 mm × 100 mm) was prepared by pouring and casting the cement mortar (water–cement ratio: 0.65) into a mold. Approximately $2h$ after the vibration, a 1-mm-thick pre-made thin plastic piece was inserted into the specimen, and then pulled out vertically to form an empty joint in the specimen after about $12h$. The specimens were cured in the curing room at 20°C and 95% relative humidity for 28 days before they were tested.

2.2. Test sequence

(1) Uniaxial compression test of intact specimens

Three intact specimens were subjected to uniaxial compression test at a 1 kN/s loading rate, to obtain their uniaxial compressive strength (σ_c), which provides the basis for determining normal stress in the direct shear test. The uniaxial compressive strengths of these intact specimens were 15.34, 15.29, and 14.79 MPa, averaged at 15.14 MPa.

(2) Shear test of specimens with a stepped joint plane

Next, the specimens with a stepped joint plane were subjected to a shear stress, yielding four categories of normal stress: $0.2\sigma_c$, $0.3\sigma_c$, $0.4\sigma_c$, and $0.5\sigma_c$, corresponding to 3.03, 4.54, 6.05, and 7.57 MPa. The shear test under each normal stress was repeated three times, the average of their shear strength values was calculated. In this test, the normal and tangential loading rates were both 1 kN/s.

2.3. Shear test group

(1) Shear test of specimens with a single-ladder step joint

Figure 1 shows a shear test diagram for specimens with a single-ladder step joint.
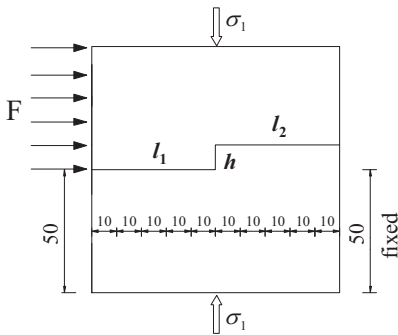
Fig. 1. Shear test diagram for specimens with a single-ladder step joint (unit: mm)

In Figure 1, l_1, l_2, and h indicate the respective lengths of the bottom and top of the step joint, and its height. Two scenarios were considered for this test (Figure 1, Table 1): (1) Lengths of bottom and top of step joints (l_1 and l_2) were fixed at 50 mm, the height of joint (h) was varied at 10, 15, 20, 25, and 30 mm; (2) at a fixed value of $h = 20$ mm,

Table 1. Shear test groups of specimens with a single-ladder step joint

Study	l_1 / mm	l_2 / mm	h / mm	Normal stress / MPa	Amount of specimens
1	50	50	10	3.03, 4.54, 6.05, 7.57	12
2	50	50	15	3.03, 4.54, 6.05, 7.57	12
3	50	50	20	3.03, 4.54, 6.05, 7.57	12
4	50	50	25	3.03, 4.54, 6.05, 7.57	12
5	50	50	30	3.03, 4.54, 6.05, 7.57	12
6	20	80	20	3.03, 4.54, 6.05, 7.57	12
7	30	70	20	3.03, 4.54, 6.05, 7.57	12
8	40	60	20	3.03, 4.54, 6.05, 7.57	12
9	60	40	20	3.03, 4.54, 6.05, 7.57	12
10	70	30	20	3.03, 4.54, 6.05, 7.57	12
11	80	20	20	3.03, 4.54, 6.05, 7.57	12

l_1 = 20, 30, 40, 50, 60, 70, and 80 mm, l_2 = 80, 70, 60, 40, 30 and 20 mm. The test groups are shown in Table 1.

(2) Shear test of specimens with a single-rectangular step joint

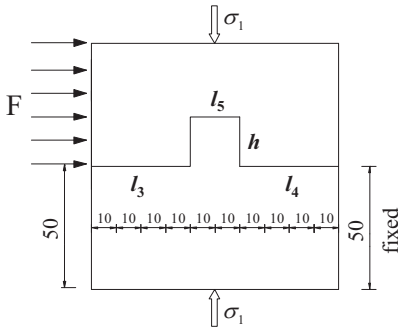Figure 2 displays a shear test diagram for specimens with a single-rectangular step joint.

Fig. 2. Shear test diagram for specimens with a single-rectangular step joint (unit: mm)

In Figure 2, l_3 and l_4 respectively indicate distances from the left lower corner of the single-rectangular step joint to the left side of the specimen and from the right lower corner of the single-rectangular step joint to the right side of the specimen. Additionally, l_5 indicates the length of the top of the single-rectangular step joint, and h indicates the step-joint height.

Three cases were considered for this test (Figure 2, Table 2): (1) Length l_3 and l_4 were fixed at 40 mm and length l_5 was 20 mm, h was changed within 10, 15, 20, 25, and 30 mm; (2) at fixed values of $l_3 = l_4$ = 10, 20, 30 and 40 mm, h = 20 mm, l_5 = 20, 40, 60, and

Table 2. Shear test groups of specimens with a single-rectangular step joint

Study	l_3 / mm	l_4 / mm	l_5 / mm	h / mm	Normal stress / MPa	Amount of specimens
1	40	40	20	10	3.03, 4.54, 6.05, 7.57	12
2	40	40	20	15	3.03, 4.54, 6.05, 7.57	12
3	40	40	20	20	3.03, 4.54, 6.05, 7.57	12
4	40	40	20	25	3.03, 4.54, 6.05, 7.57	12
5	40	40	20	30	3.03, 4.54, 6.05, 7.57	12
6	10	10	80	20	3.03, 4.54, 6.05, 7.57	12
7	20	20	60	20	3.03, 4.54, 6.05, 7.57	12
8	30	30	40	20	3.03, 4.54, 6.05, 7.57	12
9	20	60	20	20	3.03, 4.54, 6.05, 7.57	12
10	30	50	20	20	3.03, 4.54, 6.05, 7.57	12
11	50	30	20	20	3.03, 4.54, 6.05, 7.57	12
12	60	20	20	20	3.03, 4.54, 6.05, 7.57	12

80 mm; (3) at fixed values of $l_5 = 20$ mm and $h = 20$ mm, l_3 and l_4 were variable. The test groups are shown in Table 2.

(3) Shear test of specimens with a double-rectangular step joint

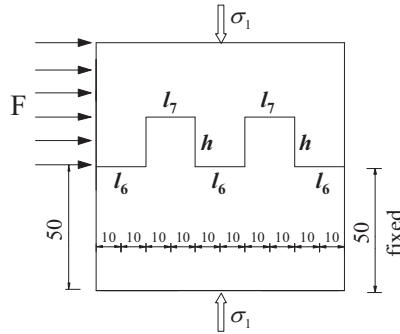Figure 3 shows a shear diagram for specimens with a double-rectangular step joint.

Fig. 3. Shear test diagram for specimens with a double-rectangular
step joint (unit: mm)

In Figure 3, l_6 and l_7 indicate the respective lengths of the bottom and top of the step joint, and h is its height. In this test, the value of l_6 and l_7 were fixed at 20 mm, and $h = 10$, 15, 20, 25, and 30 mm (Figure 3). The test groups are shown in Table 3.

Table 3. Shear test groups of specimens with a double-rectangular step joint

Study	l_6 / cm	l_7 / cm	h / cm	Normal stress / MPa	Amount of specimens
1	2.0	2.0	1.0	3.03, 4.54, 6.05, 7.57	12
2	2.0	2.0	1.5	3.03, 4.54, 6.05, 7.57	12
3	2.0	2.0	2.0	3.03, 4.54, 6.05, 7.57	12
4	2.0	2.0	2.5	3.03, 4.54, 6.05, 7.57	12
5	2.0	2.0	3.0	3.03, 4.54, 6.05, 7.57	12

In this test, the result of any one specimen exceeds 15% was excluded, and the average strength was calculated based on the other two specimens. This method was proved to be validity in Xiong et al. [16].

3. Shear test results for intact specimens

The shear strength of specimen increases gradually with normal stress from 3.03 MPa to 7.57 MPa (Figure 4). More particularly, such an increase in shear strength is visible from 3.03 MPa to 6.05 MPa and less noticeable from 6.05 MPa to 7.57 MPa.
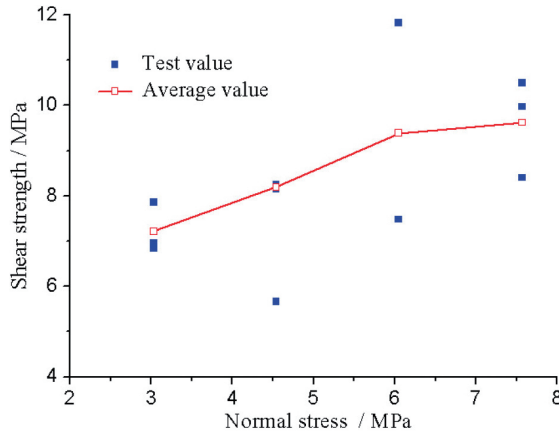
Fig. 4. Shear strengths of intact specimens

4. Shear test results of specimens with a single-ladder step joint

4.1. Analysis of shear strength

Figure 5 displays the shear strengths of specimens with a single-ladder step joint when $l_1 = l_2 = 50$ mm and $h = 10, 15, 20, 25$, and 30 mm. In this figure, the shear strength tends to increase and then decrease, reaching a maximum value at $h = 25$ mm. Figure 6 shows the shear strengths of specimens with a single-ladder step joint, given a fixed value
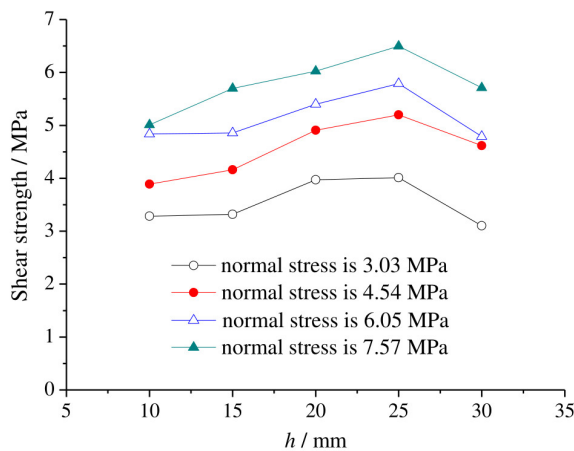
Fig. 5. Shear strengths of specimens with a single-ladder step joint
with fixed $l_1 = l_2 = 50$ mm and variable h

of $h = 20$ mm and a variable $l_1 = 20, 30, 40, 50, 60, 70$, and 80 mm. The shear strength of specimen decreases gradually with further increases in l_1.
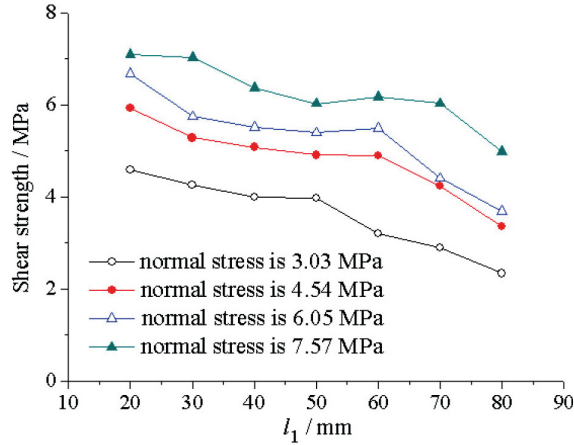
Fig. 6. Shear strengths of specimens with a single-ladder step joint
with fixed $h = 20$ mm and variable l_1

4.2. Damage morphology

Figures 7 and 8 display the post-shear-test damage morphology in specimens with a single-ladder step joint after being subjected to the shear test, assuming fixed $l_1 = l_2 = 50$ mm and variable h.

(a) normal stress is 3.03 MPa   (b) normal stress is 4.54 MPa   (c) normal stress is 6.05 MPa   (d) normal stress is 7.57 MPa

Fig. 7. Post-shear-test damage morphology in specimens with a single-ladder step joint,
given fixed $l_1 = l_2 = 50$ mm and $h = 10$ mm

When $h = 10$ mm and the normal stress is 3.03 MPa, there are seldom cracks generated with the specimen breaking, eventually causing direct shear failure. With an increase in normal stress, oblique cracks appear at the bottom and apex points of the step joints. Furthermore, when $h = 15, 20, 25$, and 30 mm and the normal stress is 3.03 MPa, oblique cracks appear at the bottom point but are seldom generated at the apex point.

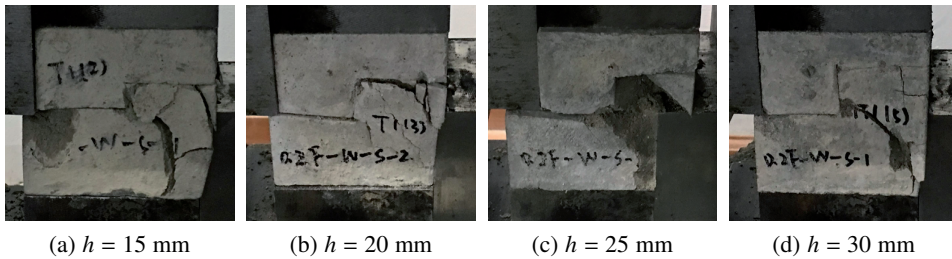(a) $h = 15$ mm   (b) $h = 20$ mm   (c) $h = 25$ mm   (d) $h = 30$ mm

Fig. 8. Post-shear-test damage morphology in specimens with a single-ladder step joint,
given fixed $l_1 = l_2 = 50$ mm and normal stress of 3.03 MPa

Figures 9 and 10 display the post-shear-test damage morphology in specimens with a single-ladder step joint under normal stresses of 3.03 and 7.57 MPa, respectively, given fixed $h = 20$ mm and variable $l_1 = 20, 40, 60$ and 80 mm. Under normal stress of 3.03 MPa, when l_1 is small, oblique cracks occur at the bottom and apex points of the step joint, causing the surface of the specimen to partially fall off. Similarly, when l_1 is large, oblique cracks are generated at the bottom and apex points; nevertheless, the number of cracks is not as large as when l_1 is small.

(a) $l_1 = 20$ mm   (b) $l_1 = 40$ mm   (c) $l_1 = 60$ mm   (d) $l_1 = 80$ mm
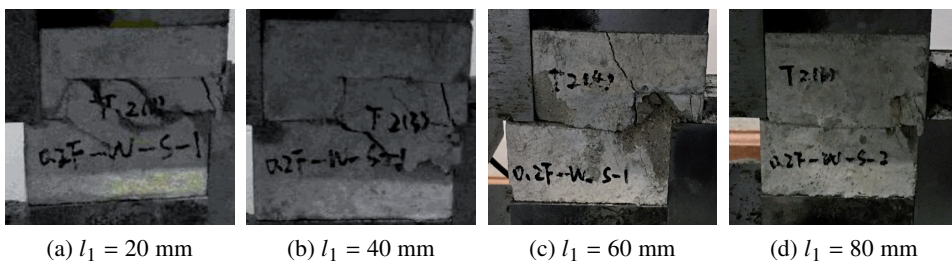
Fig. 9. Post-shear-test damage morphology in specimens with a single-ladder step joint
under normal stress of 3.03 MPa, given $h = 20$ mm and variable l_1

(a) $l_1 = 20$ mm   (b) $l_1 = 40$ mm   (c) $l_1 = 60$ mm   (d) $l_1 = 80$ mm
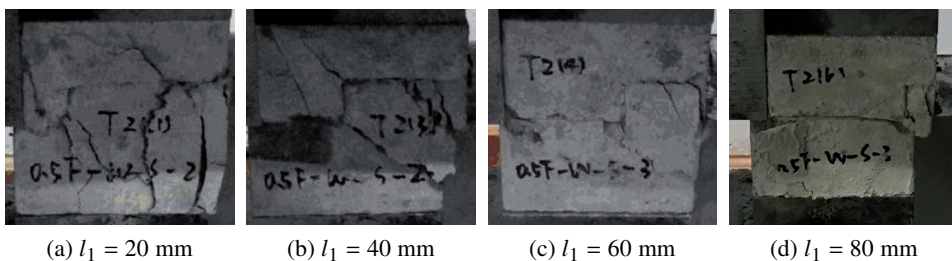
Fig. 10. Post-shear-test damage morphology in specimens with a single-ladder step joint
under normal stress of 7.57 MPa, given fixed $h = 20$ mm and variable l_1

Moreover, for specimens with a small l_1, the number of cracks before specimen breakage would increase with greater normal stress. Otherwise, for those with large l_1, the number of cracks before specimen breakage would decrease with an increase in normal stress, although such a decline might not be significant.

On the basis of Figures 9 and 10, a smaller l_1 would generate more cracks before the specimen breaks. Additionally, the frictional sliding force in these cracks would results in an increase in the shear strength of specimen.

5. Shear test results of specimens with a single-rectangular step joint

5.1. Analysis of shear strength

Figure 11 displays the shear strengths of specimens with a single-rectangular step joint, given $l_3 = l_4 = 40$ mm, $l_5 = 20$ mm, and $h = 10, 15, 20, 25$, and 30 mm. Under different normal stresses, the shear strength of specimens with a single-rectangular step joint follows a type – W variation with h, reaching a minimum at $h = 25$ mm. Generally, the specimen shear strength increases with normal stress.
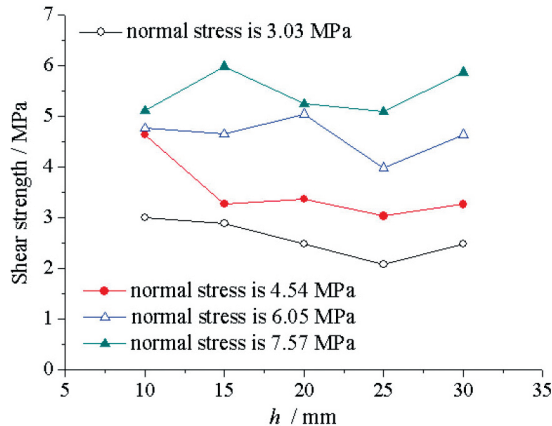

Fig. 11. Variation of shear strength with h in specimens with a single-rectangular step joint, given $l_3 = l_4 = 40$ mm and $l_5 = 20$ mm

Figure 12 displays the shear strengths of the specimens, given $l_3 = l_4$ and $h = 20$ mm, and $l_5 = 20, 40, 60$, and 80 mm. A decrease in l_5 causes a corresponding gradual decrease in the length of the rock bridge and the shear strength of the specimen.

Figure 13 displays the shear strengths in specimens with a single-rectangular step joint, assuming fixed values of $l_5 = 20$ mm and $h = 20$ mm, and variable l_3 and l_4. Under different normal stresses, the shear strength of specimen varies with an increase with l_3, reaching its maximum value at $l_3 = 50$ mm, under normal stresses of 3.03 and 4.54 MPa.
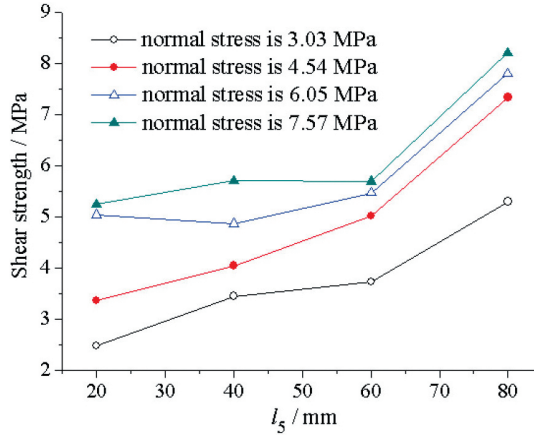
Fig. 12. Variation of shear strength with l_5 in specimens with a single-rectangular step joint, given $l_3 = l_4$ and $h = 20$ mm

Likewise, at 6.05 and 7.57 MPa, the shear strength of specimen is maximum at $l_3 = 40$ mm and $l_3 = 20$ mm, respectively.
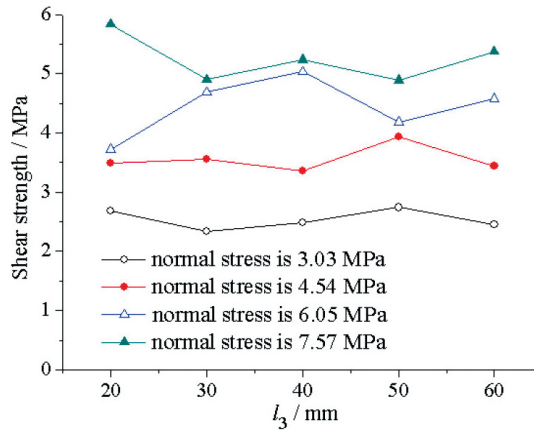

Fig. 13. Variation of shear strength with l_3 in specimens with a single-rectangular step joint, given $l_5 = 20$ mm and $h = 20$ mm

5.2. Damage morphology

Figures 14 and 15 display the post-shear-test damage morphology in specimens with a single-rectangular step joint, assuming variable h, $l_3 = l_4 = 40$ mm, and $l_5 = 20$ mm. When $h = 10$ mm and the normal stress was 3.03 MPa, crushing damage mainly occurs in the rectangular step joint. With an increase in normal stress, the crushing damage further develops in the rectangular step joint, but with less pronounced oblique cracks initiating in

the upper-right corner of the joint. Given the same normal stress, a higher h would cause the specimen to develop more oblique cracks at the upper-right and lower-left corners of the rectangular step joint. In particular, oblique cracks connect the upper-left and lower-right corners at an earlier stage. These cracks would more likely appear with greater normal stress.
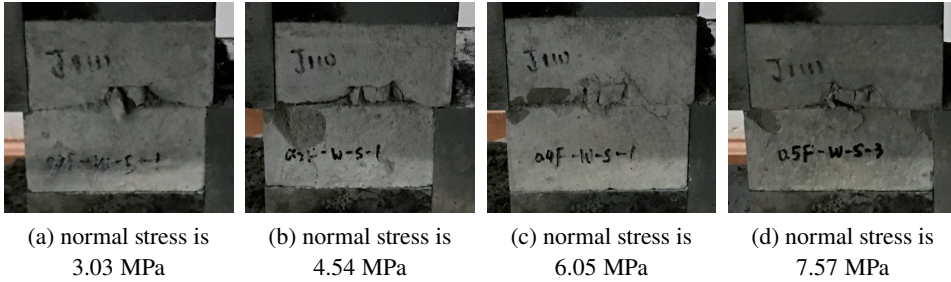

| (a) normal stress is | (b) normal stress is | (c) normal stress is | (d) normal stress is |
| 3.03 MPa | 4.54 MPa | 6.05 MPa | 7.57 MPa |

Fig. 14. Post-shear-test damage morphology in specimens with a single-rectangular step joint, given fixed $l_3 = l_4 = 50$ mm and $h = 10$ mm

| (a) $h = 15$ mm | (b) $h = 20$ mm | (c) $h = 25$ mm | (d) $h = 30$ mm |
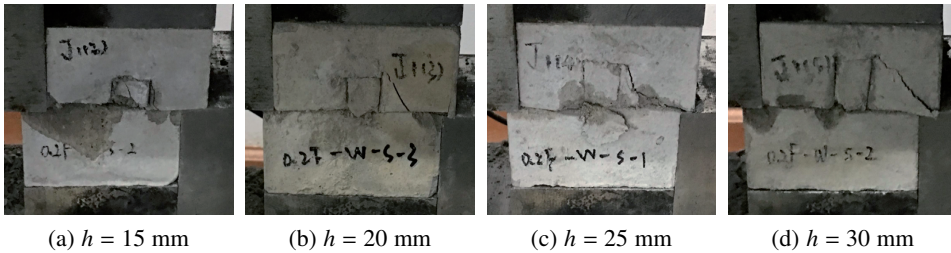
Fig. 15. Post-shear-test damage morphology in specimens with a single-ladder step joint, given fixed $l_3 = l_4 = 50$ mm and normal stress of 3.03 MPa

Figures 16 and 17 show the post-shear-test damage morphology in specimens with a single-rectangular step joint, given $l_3 = l_4$, $h = 20$ mm under normal stresses of 3.03 and 7.57 MPa. Under the same normal stress, as l_5 decreases from 80 to 20 mm, few cracks

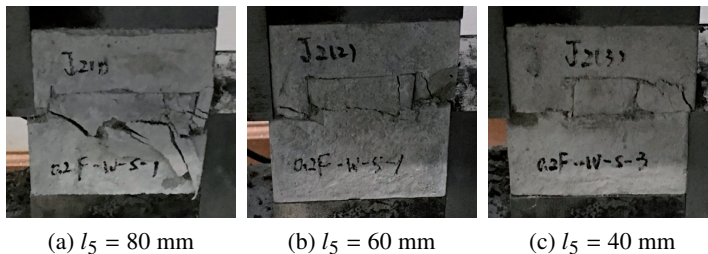| (a) $l_5 = 80$ mm | (b) $l_5 = 60$ mm | (c) $l_5 = 40$ mm |

Fig. 16. Post-shear-test damage morphology in specimens with a single-ladder step joint, given fixed $l_3 = l_4$, $h = 20$ mm and normal stress of 3.03 MPa

are generated before the failure of the specimen, the frictional sliding force in these cracks weakens, and the shear strength of the specimen decreases gradually. With greater normal stress and a fixed value of l_5, the number of cracks generates before specimen breakage gradually increases. The frictional sliding force in these cracks increases gradually with the specimen shear strength.
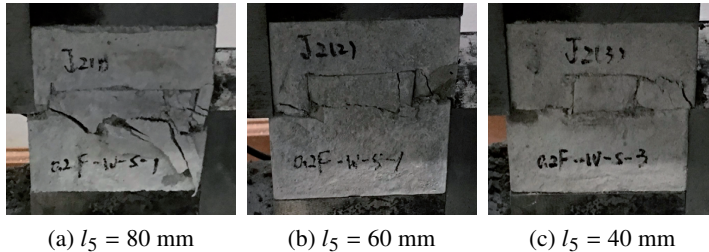

(a) $l_5 = 80$ mm   (b) $l_5 = 60$ mm   (c) $l_5 = 40$ mm

Fig. 17. Post-shear-test damage morphology in specimens with a single-ladder step joint, given fixed $l_3 = l_4$, $h = 20$ mm and normal stress of 7.57 MPa

Figure 18 displays the post-shear-test damage morphology in specimens with a single-rectangular step joint, given $l_5 = 20$ mm, $h = 20$ mm, variable l_3, under normal stresses of 3.03 MPa. Under the same normal stress, assuming $l_5 = 20$ mm and $h = 20$ mm, and $l_3 = 20, 30, 50$, and 60 mm, there is no obvious difference in crack type before specimen breakage.
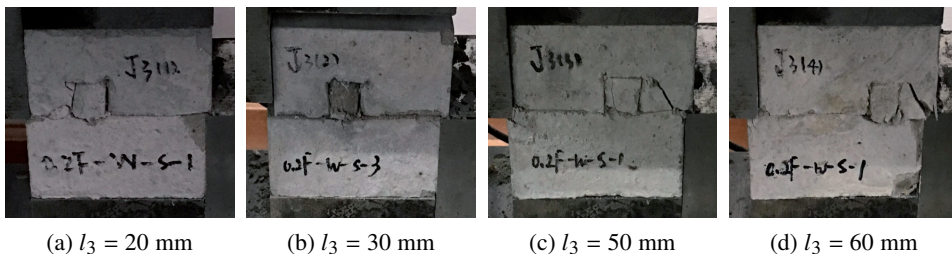

(a) $l_3 = 20$ mm   (b) $l_3 = 30$ mm   (c) $l_3 = 50$ mm   (d) $l_3 = 60$ mm

Fig. 18. Post-shear-test damage morphology in specimens with a single-rectangular step joint, given $l_5 = 20$ mm and normal stress of 3.03 MPa

6. Shear test results of specimens with a double-rectangular step joint

6.1. Analysis of shear strength

Figure 19 shows the shear strength in specimens with a double-rectangular step joint, given $l_6 = l_7 = 20$ mm and $h = 10, 15, 20, 25$, and 30 mm.
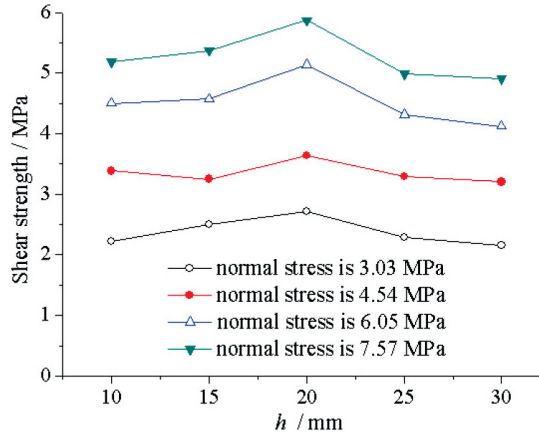
Fig. 19. Variation of shear strength of specimens with h with a double-rectangular step joint, given $l_6 = l_7 = 20$ mm

Under different normal stresses, the shear strength of specimen increases initially and then decreases with higher h, reaching its maximum value at $h = 20$ mm. Thus, with variable h, an increase in the normal stress of the specimens would tend to increase their shear strength as well.

6.2. Damage morphology

Figures 20 and 21 reflect the post-shear-test damage morphology of the same specimens at $l_6 = l_7 = 20$ mm and variable h. Under normal stress of 3.03, 4.54, 6.05, and 7.57 MPa, when $h = 10$ mm, crushing damage mainly occurs in the rectangular step joint. As h increases gradually from 15 mm under the same normal stress, oblique cracks appear frequently at the upper corner of the rectangular step joint, and triggers a likelihood of the occurrence of oblique cracks in the direction between the upper-left and lower-right corners
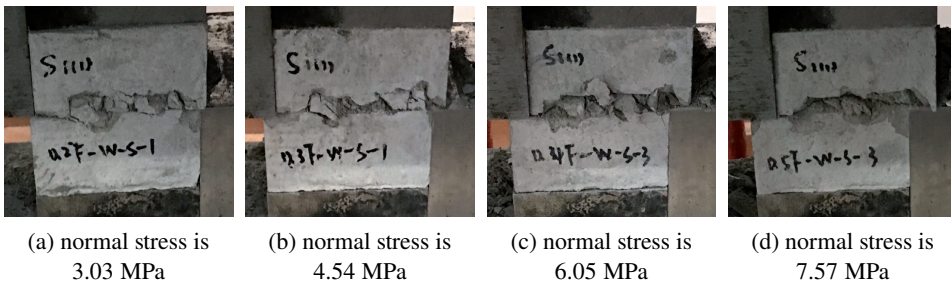
(a) normal stress is   (b) normal stress is   (c) normal stress is   (d) normal stress is
    3.03 MPa   4.54 MPa   6.05 MPa   7.57 MPa

Fig. 20. Post-shear-test damage morphology in specimens with a single-rectangular step joint, given fixed $l_3 = l_4 = 50$ mm and $h = 10$ mm

of each rectangular step joint, and oblique cracks in the direction between the upper-right corner of the left-rectangular step joint and the lower-left corner of the right-rectangular step joint. These cracks are more likely to occur with higher normal stress.
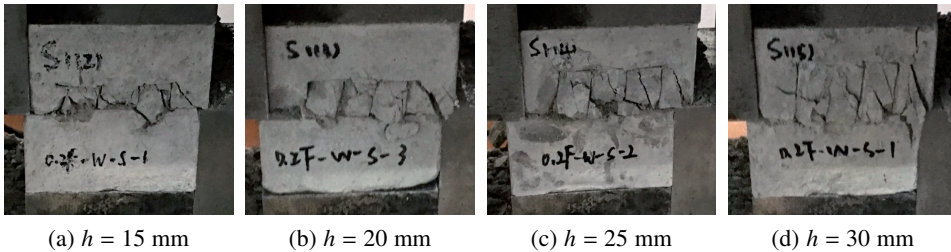

| (a) $h = 15$ mm | (b) $h = 20$ mm | (c) $h = 25$ mm | (d) $h = 30$ mm |

Fig. 21. Post-shear-test damage morphology in specimens with a single-ladder step joint, given fixed $l_3 = l_4 = 50$ mm and normal stress of 3.03 MPa

7. Comparative analysis of the shear strength of specimens with three kinds of step joint

The shear strengths of specimens with a single-ladder step joint, a single-rectangular step joint, and a double-rectangular step joint are compared when $h = 20$ mm. Three scenarios were considered for specimens with a single-ladder step joint: (1) $h = 20$ mm, $l_1 = 20$ mm; (2) $h = 20$ mm, $l_1 = 40$ mm; (3) $h = 20$ mm, $l_1 = 60$ mm. Likewise, three cases were allocated for specimens with a single-rectangular step joint: (1) $h = 20$ mm, $l_3 = 20$ mm; (2) $h = 20$ mm, $l_3 = 40$ mm; (3) $h = 20$ mm, $l_3 = 60$ mm. Only the case $h = 20$ mm and $l_6 = l_7 = 20$ mm is taken for specimens with a double-rectangular step joint. The comparison results are provided in Figure 22.

single-ladder step joint: $h = 20$ mm, $l_1 = 20$ mm
single-ladder step joint: $h = 20$ mm, $l_1 = 40$ mm
single-ladder step joint: $h = 20$ mm, $l_1 = 60$ mm
single-rectangular step joint: $h = 20$ mm, $l_3 = 20$ mm
single-rectangular step joint: $h = 20$ mm, $l_3 = 40$ mm
single-rectangular step joint: $h = 20$ mm, $l_3 = 60$ mm
double-rectangular step joint: $h = 20$ mm, $l_6 = l_7 = 20$ mm
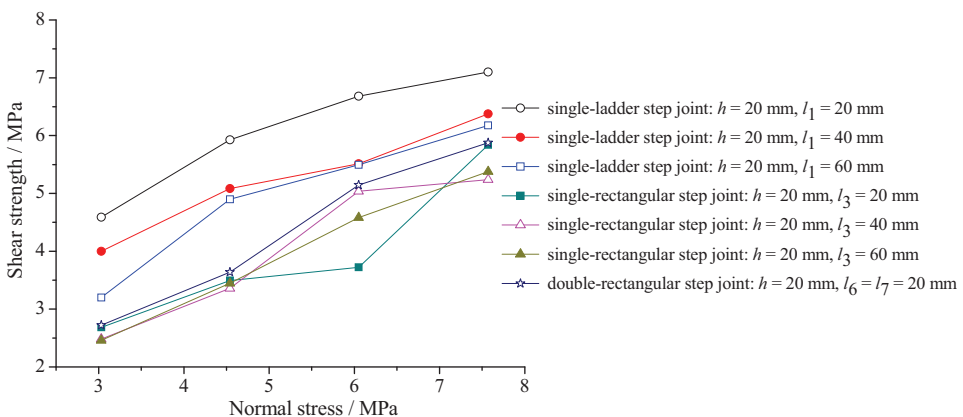
Fig. 22. Comparison results of the shear strength in specimens with three kinds of step joint

Specimens with a single-ladder step joint have the highest shear strength, mainly because the length of the rock bridge in the straight shear direction is the highest. The shear strength of specimens with a double-rectangular step joint is higher than that of specimens with a single-rectangular step joint. Under the same normal stress, specimens with a double-rectangular step joint have a larger number of cracks before breakage than those with a single-ladder step joint. Moreover, the rock bridge in specimens with a double-rectangular step joint in the straight shear direction is longer than that in specimens with a single-ladder step joint.

8. Conclusions

1. When the lengths of the top and bottom of the step joint for specimens with a single-ladder step joint are assumed to be constant, any increase in h (the height of the joint) would cause a corresponding initial increase and subsequent decrease in the shear strength.
2. For specimens with a single-ladder step joint, a small h and a relatively low normal stress would make it difficult to generate cracks in the specimens before their breakage, resulting in direct shear failure. Moreover, with a further increase in normal stress, oblique cracks would tend to appear at the bottom and apex points of the step joint.
3. For specimens with a single-rectangular step joint under different normal stresses, any increase in h would produce a type-W variation pattern with h. At constant h, gradual decrease in the length of the rock bridge would cause a gradual decrease in the shear strength of specimen.
4. For specimens with a single-rectangular step joint, small values of h and low normal stress would allow a crushing damage which mainly occurs in the step joint. Any further increases in the normal stress would allow, in addition to the crushing damage, the appearance of less pronounced oblique cracks in the upper-right corner of the step joint. Under the same normal stress, a higher h would entertain the likelihood of oblique cracks appearing in the upper-right and lower-left corners of the rectangular step joint.
5. For specimens with a double-rectangular step joint subjected to the same normal stress, any increase in h would cause an initial-increase–decrease tendency for the shear strength. For small h, a crushing damage would mainly occur in the rectangular step joint. Moreover, under the same normal stress, an increase in h allows an oblique crack to form easily at the upper corner of the rectangular step joints.
6. A constant h would cause maximum shear strength in specimens with a single-ladder step joint, followed by specimens with a double-rectangular step joint. By contrast, the shear strength of specimens with a single-rectangular step joint would be the least.

Acknowledgements

References

[1] Z.Y. Yang, D.Y. Chiang, "An experimental study on the progressive shear behavior of rock joints with tooth-shaped asperities", *International Journal of Rock Mechanics & Mining Sciences*, 2000, vol. 37, pp. 1247–1259; DOI: 10.1016/S1365-1609(00)00055-1.

[2] A.H. Ghazvinian, A. Taghichian, M. Hashemi, et al., "The shear behavior of bedding planes of weakness between two different rock types with high strength difference", *Rock Mechanics and Rock Engineering*, 2010, vol. 43, pp. 69–87; DOI: 10.1007/s00603-009-0030-8.

[3] S.A. Mohammad, R. Vamegh, B. Giovanni, "A bonded particle model simulation of shear strength and asperity degradation for rough rock fractures", *Rock Mechanics and Rock Engineering*, 2012, vol. 45, pp. 649–675; DOI: 10.1007/s00603-012-0231-4.

[4] Z.M. He, Z.Y. Xiong, Q.G. Hu, et al., "Analytical and numerical solutions for shear mechanical behaviors of structural plane", *Journal of Central South University of Technology*, 2014, vol. 21; DOI: 10.1007/s11771-014-2261-4.

[5] M. Bahaaddini, P.C. Hagan, R. Mitra, et al., "Experimental and numerical study of asperity degradation in the direct shear test", *Engineering Geology*, 2016, vol. 204, pp. 41–52; DOI: 10.1016/j.enggeo.2016.01.018.

[6] S.M. Mahdi Niktabar, K. Seshagiri Rao, A.K. Shrivastava, "Effect of rock joint roughness on its cyclic shear behavior", *Journal of Rock Mechanics and Geotechnical Engineering*, 2017, vol. 9, no. 6, pp. 1071–1084; DOI: 10.1016/j.jrmge.2017.09.001.

[7] Y.C. Tian, Q.S. Liu, H. Ma, et al., "New peak shear strength model for cement filled rock joints", *Engineering Geology*, 2018, vol. 233, pp. 269–280; DOI: 10.1016/j.enggeo.2017.12.021.

[8] X.B. Zhang, Q.H. Jiang, P.H.S.W. Kulatilake, et al., "Influence of asperity morphology on failure characteristics and shear strength properties of rock joints under direct shear tests", *International Journal of Geomechanics*, 2019, vol. 19, pp. 1–13; DOI: 10.1061/(ASCE)GM.1943-5622.0001347.

[9] L.X. Xiong, H.J. Chen, Y. Zhang, "Direct shear tests of arti?cial jointed rock specimens with parallel joints", *Arabian Journal of Geosciences*, 2020, vol. 13, art. ID 373; DOI: 10.1007/s12517-020-05424-5.

[10] L.X. Xiong, H.J. Chen, Y. Zhang, "Shear mechanical properties of artificial rock specimen with symmetrical and asymmetric toothed structural joints", *Indian Geotechnical Journal*, 2021, vol. 51, pp. 347–358; DOI: 10.1007/s40098-020-00455-x.

[11] B.Y. Hao, L.X. Xiong, Y.L. Li, et al., "Cyclic direct shear test on rock sample with stepped structural plane", *Geotechnical and Geological Engineering*, 2021, vol. 39, pp. 2373–2397; DOI: 10.1007/s10706-020-01633-7.

[12] X.X. Yang, P.H.S.W. Kulatilake, "Laboratory investigation of mechanical behavior of granite samples containing discontinuous joints through direct shear tests", *Arabian Journal of Geosciences*, 2019, vol. 12, art. ID 79; DOI: 10.1007/s12517-019-4278-3.

[13] Y.F. Cui, "Effect of joint type on the shear behavior of synthetic rock", *Bulletin of Engineering Geology and the Environment*, 2019, vol. 78, pp. 3395–3412; DOI: 10.1007/s10064-018-1325-3.

[14] L.X. Xiong, H.J. Chen, X.L. Geng, et al., "Influence of joint location and connectivity on the shear properties of arti?cial rock samples with non-persistent planar joints", *Arabian Journal of Geosciences*, 2020, vol. 13, art. ID 565; DOI: 10.1007/s12517-020-05589-z.

[15] T.H. Kwon, E.S. Hong, G.C. Cho, "Shear behavior of rectangular-shaped asperities in rock joints", *KSCE Journal of Civil Engineering*, 2010, vol. 14, pp. 323–332; DOI: 10.1007/s12205-010-0323-1.

[16] L.X. Xiong, H.J. Chen, "Effects of high temperatures and loading rates on the splitting tensile strength of jointed rock mass", *Geotechnical and Geological Engineering*, 2020, vol. 38, pp. 1885–1898; DOI: 10.1007/s10706-019-01137-z.